Plastic Limit Pressures of Circumferential Cracked Pipe Bends

Seok-Pyo Hong[1,a], Jong-Hyun Kim[1,b] and Yun-Jae Kim[1,c]

[1] Mechanical Engineering, Korea University, Seoul, Korea

[a]seok-pyo@korea.ac.kr, [b]bapa@korea.ac.kr, [c]kimy0308@korea.ac.kr

Keywords: Circumferential part-through surface and through-wall cracks, Finite element limit analysis, Limit pressure, Pipe Bend

Abstract. This paper provides limit pressures for circumferential cracked pipe bends, resulting from systematic, small strain FE limit analyses using elastic-perfectly plastic materials. Circumferential through-wall and constant-depth part-through surface cracks at both extrados and intrados are considered, but the length of circumferential through-wall cracks is limited to 50% of the circumference. It is found that limit pressures of pipe bends are not affected by the presence of the circumferential surface crack, unless it is sufficiently deep and long. Moreover limit pressures for circumferential surface cracked pipe bend decrease almost linearly with increasing a/t and θ/π. Based on FE results, approximate closed-form solutions for limit pressures are given.

Introduction

Plastic limit analysis of pressurized pipes with circumferential cracks has been an important issue in the field of structural integrity assessment, due to its importance in design and assessment. For instance, plastic loads obtained from plastic limit analyses can be directly used to estimate maximum load-carrying capacities, see e.g. Ref. [1]. Furthermore, based on the reference stress approach [2], it can be used to estimate non-linear fracture mechanics parameters such as J and C^* integrals (see for instance Refs. [3-5]). As pressurized pipes are typically subject to system loadings such as bending, plastic limit analysis needs to be performed for combined loadings. For instance, for circumferential cracked straight pipes under combined loadings, extensive analytical, experimental and numerical results have been reported up to present, resulting in closed-form plastic limit load solutions. Accordingly numerous publications can be found in the literature, and interesting readers can refer to, for instance, Refs. [6-11].

Typical pipeworks include not only straight pipes but also pipe bends, and thus plastic limit analyses of circumferential cracked pipe bends need to be performed. Numerous papers related to plastic limit analyses of circumferential cracked pipe bends have been reported in literature, resulting from analytical, experimental and numerical works. Reviewing literatures is exhaustive and is not within the scope of this paper. Here only works relevant to the present paper are summarized here, that is, those closely related to plastic limit analyses for circumferential cracked pipe bends under combined pressure and in-plane bending. Due to complexities involved in the problem, no analytical solution has been yet reported. Experimental results were reported for pipe bends with circumferential through-wall and part-through wall cracks by a number of researchers [12-17]. Although experimental data are extremely valuable, data are still limited to draw systematic and concrete conclusions due to time and expense involved in full-scale tests. For instance, existing test data are mainly for pure bending loading, and thus quantification of the internal pressure effect was missing. In this respect, an attractive approach for systematic investigation on plastic limit analysis of cracked pipe bends is to use finite element (FE) method, which has been quite popular recently. For instance, Yahiaoui et al. [12,13] performed the FE limit analysis for cracked pipe bends, but their cases were still limited to draw general plastic load solutions for cracked pipe bends under combined loadings. Chattopadhay and co-workers published a number of papers on plastic limit analysis of cracked pipe bends [16-18]. They defined plastic loads by the twice-elastic-slope method (which will be referred to as “TES plastic loads”

here), and also proposed closed-form TES plastic load solutions for circumferential through-wall cracked pipes bends under combined internal pressure and bending [18]. As TES plastic load solutions were given only for circumferential through-wall cracks, those for part-through surface cracks are missing. Furthermore, they did not investigate cases of pure pressure loading.

In this paper, limit pressures of circumferential cracked pipe bends under combined pressure and in-plane bending are presented, resulting from systematic plastic limit analyses. The results are based on three-dimensional FE limit analyses using elastic-perfectly plastic materials. Both through-wall and constant-depth part-through surface cracks are considered, and two different crack locations are considered; at extrados and at intrados.

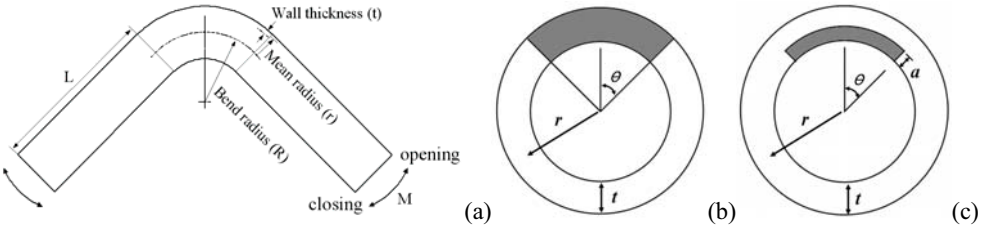

Fig. 1. Relevant variables for (a) pipe bends with attached straight pipes, (b) circumferential through wall crack, and (c) circumferential part-through surface crack.

Finite Element Limit Analyses

Geometry Figure 1a depicts a 90° pipe bend, considered in the present work. The mean radius and thickness of the pipe are denoted by r and t, respectively, and the bend radius by R, leading to non-dimensional variables, R/r and r/t. The non-dimensional bend characteristic should be also noted:

$$\lambda = \frac{Rt}{r^2} = \frac{(R/r)}{(r/t)} \tag{1}$$

To quantify the effect of the bend geometry on plastic loads, above non-dimensional variables were systematically varied. Three different values of r/t, r/t=5, 10 and 20, were considered, together with various values of R/r. For selected cases, however, higher values of r/t were also considered. The piping system considered comprised the 90° bend and the attached straight pipe of length L (Fig. 1a). Introduction of the attached straight pipe is to minimize the end effect due to the applied loading. The effect of the length of the attached straight pipe, L, on plastic behaviour is found to be minimal, as long as it is longer than four time the pipe radius, L=4r [20]. In this paper, it was chosen to be twenty times the pipe radius, L=20r.

Both circumferential through-wall and part-through surface cracks were considered. The circumferential through-wall crack is characterized by its relative crack length, θ/π, where θ denotes the half crack length (Fig. 1b). The value of θ/π was systematically varied from θ/π=0 to θ/π=0.5, which would cover interesting ranges of crack in practical situations. Furthermore, when the value of θ/π is larger than θ/π=0.5, the crack closure phenomenon could occur, which is quite complex to analyse. For circumferential part-through surface cracks, one additional geometric variable, the relative crack depth, a/t, was further considered (Fig. 1c). Note that the surface crack was assumed to have a rectangular shape (constant-depth), and the value of θ/π was limited up to θ/π=0.5. Note also that, as constant-depth surface cracks are considered, the results in the limiting case of $a/t \rightarrow 1$

should recover those for through-wall cracks. Regarding a crack location, both extrados and intrados cracks were considered in the present work.

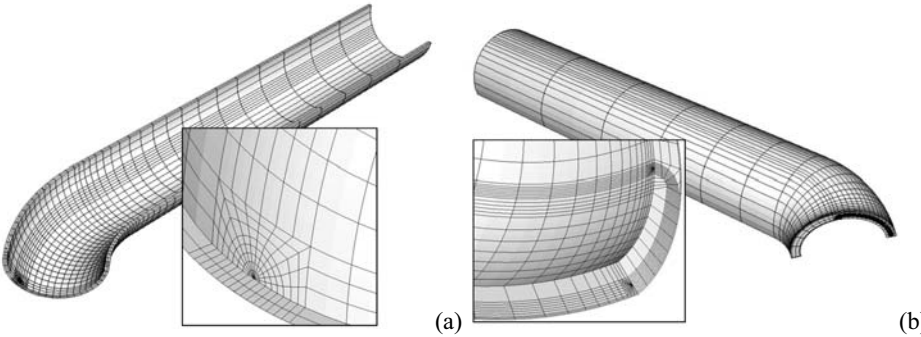

(a) (b)

Fig. 2. Typical finite element meshes for pipe bends with (a) circumferential through-wall crack, and (b) circumferential part-through surface crack.

Finite Element Analysis Figure 2 depicts typical FE meshes for pipe bends with the circumferential through-wall and part-through surface cracks, employed in the present work. The crack-tip was designed with collapsed elements, and a ring of wedge-shaped elements was used in the crack-tip region. For through-wall crack cases, two elements were used through the thickness. For part-through surface crack cases, a total of eleven or twelve elements were used through the thickness; four elements in the cracked ligament and seven to eight elements in the un-cracked ligament, which is believed to be sufficiently fine for plastic limit analyses. Plastic limit analyses of the pipe bend were performed using ABAQUS [21]. Materials were assumed to be elastic-perfectly plastic, and non-hardening J_2 flow theory was used. The following values of material properties were assumed in the present work; Young's modulus of E=200GPa, Poisson's ratio of ν=0.3, and the limiting stress of σ_o=200MPa. For efficient computation, a quarter model was used due to symmetry conditions and reduced integration elements (element type C3D20R within ABAQUS) were used. For through-wall crack cases, the number of elements and nodes in typical FE meshes were 2,028 elements/11,528 nodes. For part-through surface crack cases, they were ranged from 3,900 elements/18,000 nodes to 5,800 elements/27,000 nodes.

Only internal pressure loading is considered in the present work. As pipe bends are flexible components, the large geometry change effect on plastic behaviours could be important. However, for internal pressure, it is known that the large geometry change effect is minimal [19]. Thus limit analyses were performed using the small geometry change option. Internal pressure was applied as a distributed load to the inner surface of the FE model, together with an axial tension equivalent to the internal pressure applied at the end of the pipe to simulate closing ends. The effect of the crack face pressure was fully considered, that is, 100% of the internal pressure was applied to the crack face for part-through surface cracks, and 50% for through-wall cracks. To avoid problems associated with convergence in elastic-perfectly plastic calculations, the RIKS option within ABAQUS was invoked. Limit analyses using elastic-perfectly plastic materials with the small geometry change option give clear limiting pressures.

Limit Pressures

Un-Cracked Pipe Bends Based on FE results, the following approximation for limit pressures of 90^o pipe bends is proposed

$$P_o = \frac{2}{\sqrt{3}}\sigma_o \frac{t}{r}\cdot f$$

$$f\left(\frac{r}{t},\frac{R}{r}\right) = \frac{1}{1+\left[1.21\left(\frac{r}{t}\right)^{0.0875}-1\right]\exp\left[-\left(0.307+0.00131\frac{r}{t}\right)\frac{r}{R}\right]} \quad (2)$$

where f is a non-dimensional function to reflect reduction in limit pressures due to pipe and bend geometries. Comparison with FE results showed overall good agreements.

Through-Wall Cracked Pipe Bends For intrados through-wall cracks, FE limit pressures are shown in Fig. 3a. Note that FE limit pressures for through-wall cracked pipe bends, P_L^{FE}, are normalized with respect to FE limit pressures for un-cracked pipe bends, P_o^{FE}. It shows that values of P_L^{FE}/P_o^{FE} are almost insensitive to R/r. The dependence of P_L^{FE}/P_o^{FE} on r/t is also minor. Values of P_L^{FE}/P_o^{FE} increases slightly with decreasing r/t, and differences are the largest for θ/π=~0.3. On the other hand, the effect of θ/π on P_L^{FE}/P_o^{FE} could be significant, and is almost linear. Results in Fig. 3a suggest that the dominant variable is θ/π, and the following approximation is proposed based on FE results for r/t=20:

$$\frac{P_L}{P_o} = \min\left[1.0,\ \ 1.5-2.4\left(\frac{\theta}{\pi}\right)\right] \quad (3)$$

This is compared with FE results in Fig. 3b, showing overall good agreements. In Eq. (3), P_o denotes plastic limit pressures of un-cracked pipe bends, given by Eq. (2). The factor P_L/P_o is regarded as a weakening factor due to the presence of the crack. Results in Fig. 3 suggest that limit pressures for pipe bends are not affected by the presence of the circumferential through-wall crack when the crack length is less than ~20% of the circumference. For longer cracks, limit pressures decrease linearly with increasing θ/π. A final notable point is that Eq. (3) is valid only for $\theta/\pi \le 0.5$. Regarding the validity of r/t, FE results in Fig. 3 suggest almost no dependence on R/r and r/t, and thus Eq. (3) can be applied to higher values of r/t.

Corresponding results for extrados through-wall cracks are shown in Fig. 4. No effect of R/r on P_L^{FE}/P_o^{FE} can be seen, as for the intrados case. The effect of r/t, however, is more pronounced, particularly for moderate values of θ/π, ~0.1<θ/π<~0.4. Values of P_L^{FE}/P_o^{FE} decrease with increasing r/t, and differences are the largest for θ/π=~0.25. The reason for the r/t effect can be found from plastic zone development. For r/t=5, the plastic zone occurs not only in the extrados region where the crack is located but also in the intrados region. On the other hand, for r/t=30, it occurs only in the extrados region. Consequently the FE limit pressure for r/t=5 is higher than that for r/t=30. Although variations of P_L^{FE}/P_o^{FE} with θ/π are more complex than those for intrados cracks, the following approximation is proposed for limit pressures of pipe bends with extrados through-wall cracks:

$$\frac{P_L}{P_o} = \min\left[1.0, 1.0+\left\{1.3-0.06\left(\frac{r}{t}\right)\right\}\left(\frac{\theta}{\pi}\right)+\left\{-5.1+0.12\left(\frac{r}{t}\right)\right\}\left(\frac{\theta}{\pi}\right)^2\right] \quad (4)$$

This is compared with FE results in Fig. 4b. Again, P_o in Eq. (4) denotes plastic limit pressures of un-cracked pipe bends, and Eq. (4) is valid only for $\theta/\pi \le 0.5$. As Eq. (4) depends on r/t, the validity range for r/t should be noted. As shown in Fig. 4, present FE results cover up to the case of r/t=30, and thus Eq. (4) should be used for $r/t \le 30$. For higher values of r/t, results for r/t=50 shown in Fig.

4b suggest that limit pressures for larger *r/t* values do not depend on *r/t* anymore. Thus, Eq. (4) with *r/t*=30 can be used to estimate limit pressures for larger *r/t* values.

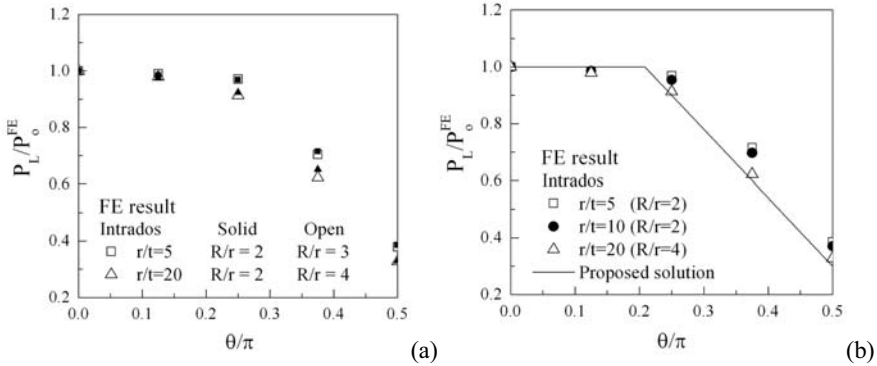

Fig. 3. Variations of P_L^{FE}/P_o^{FE} with θ/π for intrados through-wall cracks: (a) effects of R/r and r/t, and (b) comparison with the proposed approximation.

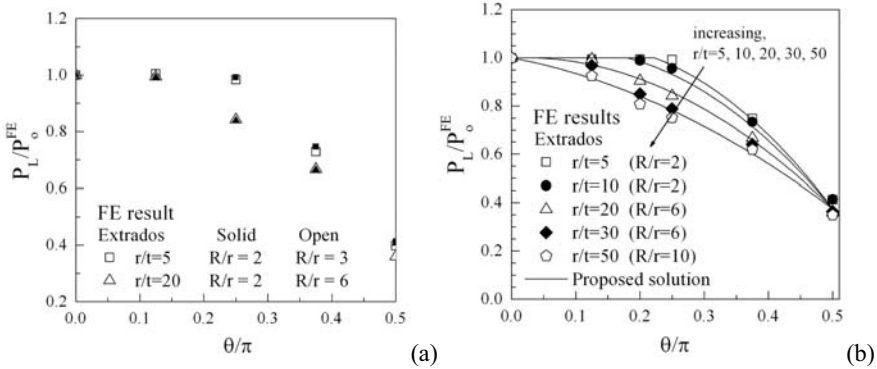

Fig. 4. Variations of P_L^{FE}/P_o^{FE} with θ/π for extrados through-wall cracks: (a) effects of R/r and r/t, and (b) comparison with the proposed approximation.

Part-Through Surface Cracked Pipe Bends Variations of FE limit pressures for intrados surface cracks with the relative crack depth *a/t* are shown in Fig. 5. As for through-wall cracks, FE limit pressures, P_L^{FE}, are normalized with respect to those for FE limit pressures for un-cracked pipe bends, P_o^{FE}. Note that results for *a/t*=1.0 correspond to those for through-wall cracks, given in the previous section. Several interesting features can be noted from the results in Fig. 5. The first one is that values of P_L^{FE}/P_o^{FE} are not so sensitive to *R/r* and *r/t*, as for through-wall cracked cases. The second point is that the limit pressure for surface cracked pipe bends is not affected by the surface crack, unless it is sufficiently long and deep. For instance, when the relative crack depth, *a/t*, is less than 0.6, the limit pressure for the cracked pipe bend is the same as that for the un-cracked pipe bend, regardless of θ/π. Moreover, when θ/π<~0.2, the limit pressure for the cracked pipe bend is practically the same as that for the un-cracked pipe bend, regardless of *a/t*. This is fully consistent to findings in Ref. [16]. The final point is that, when the surface crack is sufficiently deep and long, the dependence of P_L^{FE}/P_o^{FE} on *a/t* is practically linear. Note also that for through-wall cracks, the dependence of P_L^{FE}/P_o^{FE} on θ/π was practically linear. These observations lead to the following simple approximation for limit pressures of pipe bends with intrados surface cracks:

$$\frac{P_L}{P_o} = \min\left\{1.0,\ -3.9\left(\frac{\theta}{\pi}\right)\left(\frac{a}{t}\right)+1.5\left(\frac{\theta}{\pi}\right)+1.5\right\} \tag{5}$$

This is compared with FE results in Fig. 5, showing that it gives overall lower limit pressures than FE limit pressures and thus is conservative. In the limiting case of $a/t \rightarrow 1.0$, Eq. (5) recovers the proposed equation for through-wall cracks, Eq. (3). As for through-wall crack cases, Eq. (5) is valid only for $\theta/\pi \leq 0.5$. Regarding the validity of r/t, Eq. (5) does not depend on r/t and thus can be applied to any value of r/t.

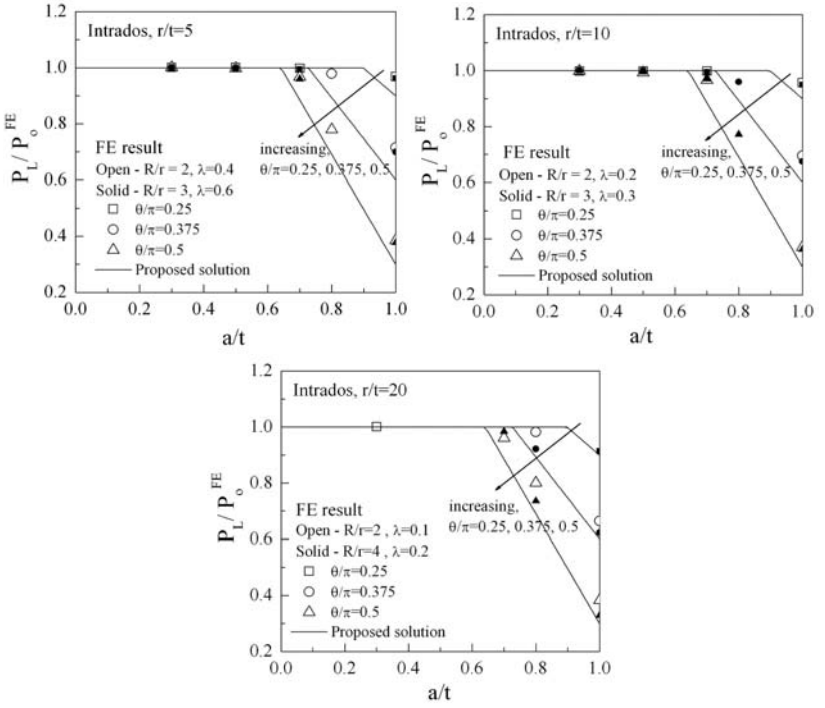

Fig. 5. Variations of P_L^{FE}/P_o^{FE} with a/t for intrados part-through surface cracks.

Corresponding results for extrados surface cracks are shown in Fig. 6. Overall trends are quite similar to those for intrados surface crack cases, shown in Fig. 5. These observations lead to the following simple approximation for limit pressures of pipe bends with extrados surface cracks:

$$\frac{P_L}{P_o} = \min\left\{1.0,\ \left[\left(-6.3+0.12\left(\frac{r}{t}\right)\right)\left(\frac{\theta}{\pi}\right)^2+\left(-0.5-0.06\left(\frac{r}{t}\right)\right)\left(\frac{\theta}{\pi}\right)\right]\left(\frac{a}{t}\right)+1.2\left(\frac{\theta}{\pi}\right)^2+1.8\left(\frac{\theta}{\pi}\right)+1\right\} \quad (6)$$

This is compared with FE results in Fig. 6. As for through-wall crack cases, Eq. (6) is valid only for $\theta/\pi \leq 0.5$ and for $r/t \leq 30$. For higher values of r/t, Eq. (6) can be used with higher degree of conservatism.

Concluding remarks

This paper provides limit pressures for circumferential cracked pipe bends, resulting from systematic, small strain FE limit analyses using elastic-perfectly plastic materials. Circumferential through-wall and constant-depth part-through surface cracks at both extrados and intrados are considered. The length of circumferential through-wall cracks is, however, limited to 50% of the

circumference. Based on FE results, approximate closed-form solutions for limit pressures are also given, which are believed to be quite general.

One interesting finding is the effect of the circumferential crack on limit pressures of pipe bends. When the depth of the circumferential crack is less than 60% of the pipe thickness, the presence of the crack does not affect the limit pressure and thus the limit pressure for the cracked pipe bend is the same as that for un-cracked pipe bend. Furthermore, even for the case of the through-wall crack, the presence of the crack does not affect the limit pressure, when its length is less than 20% of the circumference. This implies that limit pressures of pipe bends are affected by the presence of the circumferential surface crack, only when it is sufficiently deep and long. Such a finding is consistent to those reported in Ref. [16]. Another interesting point is that, for intrados cracks, limit pressures for circumferential surface cracked pipe bend decrease almost linearly with increasing a/t and θ/π, and are almost independent on elbow geometries such as R/r and r/t. For extrados cracks, effects of θ/π and r/t on limit pressures are slightly more complicated, although overall trends are quite similar to those for intrados cracks.

As information on limit pressures for cracked components has its own merit in defect assessment, present results are believed to be valuable for defect assessment of circumferential pipe bends. Furthermore present results will be valuable information to construct yield loci for cracked pipe bends under combined pressure and in-plane bending, of which results will be presented later.

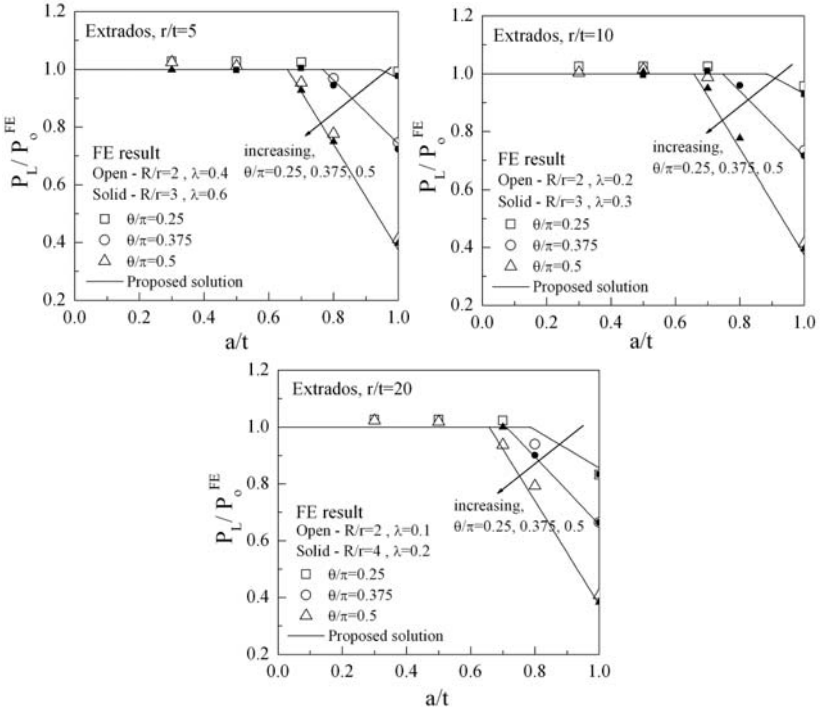

Fig. 9. Variations of P_L^{FE}/P_o^{FE} with a/t for extrados part-through surface cracks.

References

[1] ASME Boiler and Pressure Vessel Code Section III, Section XI (1992).

[2] Ainsworth RA. Engineering Fracture Mechanics 1984; 19: 633–42.

[3] R6: assessment of the integrity of structures containing defects. Revision 4, British Energy; 2001.

[4] R5: an assessment procedure for the high temperature response of structures. Issue 3, British Energy; 2003.

[5] Webster GA, Ainsworth RA. High temperature component life assessment. Chapman & Hall; 1994.

[6] Miller AG. International Journal of Pressure Vessels and Piping 1988; 32: 191–327.

[7] Oh CK, Kim YJ, Kim JS, Jin TE. Engineering Fracture Mechanics 2008; 75: 2175-2190.

[8] Kim Y-J, Shim D-J, Nikbin K, Kim Y-J, Hwang S-S, Kim J-S. International Journal of Pressure Vessels and Piping 2003; 80: 527-40.

[9] Oh C-S, Song T-K, Kim Y-J. Fatigue and Fracture of Engineering Materials and Structures 2007; 30: 1127-1244.

[10] Lei Y, Budden PJ. Journal of Strain Analysis 2004; 39: 673-683.

[11] Oh C-K, Kim Y-J, Kim J-S, Jin T-E. Engineering Fracture Mechanics 2008; 75: 2175-2190..

[12] Griffiths JE. International Journal of Mechanical Sciences 1979; 21: 119-130.

[13] Yahiaoui K, Moffat DG, Moreton DN. Journal of Strain Analysis 2000; 35: 47-57.

[14] Yahiaoui K, Moffat DG, Moreton DN. Journal of Strain Analysis 2000; 35: 47-57.

[15] Yahiaoui K, Moreton DN, Moffat DG. International Journal of Pressure Vessels and Piping 2002; 79: 27-36.

[16] Chattopadhyay J, Tomar AKS, Dutta BK, Kushwaha HS. Fatigue and Fracture of Engineering Materials and Structures 2004; 27: 1091-1103.

[17] Chattopadhyay J, Pavankumar TV, Dutta BK, Kushwaha HS. Engineering Fracture Mechanics 2005; 72: 1461-1497.

[18] Chattopadhyay J, Tomar AKS. Engineering Fracture Mechanics 2006; 73: 829-854.

[19] Robertson A, Li H, Mackenzie D. International Journal of Pressure Vessels and Piping 2005; 82: 407-16.

[20] Kim YJ, Oh CS. International Journal of Pressure Vessels and Piping, 2007, 84, 177-184.

[21] ABAQUS Version 6.2-1. User's manual. Hibbitt, Karlsson and Sorensen, Inc, RI; 2001.